

Pairing by disorder of dopants in a magnetic spin ladder

K. Knakkegaard Nielsen¹

¹Max-Planck Institute for Quantum Optics, Hans-Kopfermann-Str. 1, D-85748 Garching, Germany

(Dated: July 2, 2024)

I demonstrate a pairing mechanism of dopants in a magnetic lattice, emerging from the underlying *high-temperature disorder* of the spins. The effect is demonstrated in a mixed-dimensional model, where dopants travel along a two-leg ladder, while the spins feature Ising interactions along the rungs and the legs of the ladder. The dynamics following the sudden immersion of two nearest neighbor dopants in an infinite temperature spin lattice shows that thermal spin disorder frustrates the relative motion of the dopants and enforces them to co-propagate. The predictions are shown to be realistically testable in quantum simulation experiments.

Understanding pairing of dopants in magnetic lattices is an immense challenge in modern quantum many-body theory. The main goal is to gain a deeper understanding of strongly correlated systems, arising e.g. in the notoriously difficult high-temperature superconductors [1–3]. While solid state experiments continue to pursue such inquiries after decades of research [4], a highly interesting and promising pathway has appeared in quantum simulation experiments with ultracold atoms in optical lattices [5–12]. Single-site resolution capabilities [13, 14] makes it possible to measure low-temperature spatial correlations [8–11], as well as track them over time by repeated realizations of the same initial state. In particular, single hole dynamics consistent with magnetic polaron formation [15] in quantum antiferromagnets has been measured [6]. Moreover, in such experiments one can tinker with the simulated models, otherwise fixed in the solid state. This has enabled the observation of dopant pairing in a mixed-dimensional magnetic lattice [12]. This has also been seen to be a plausible explanation [17] for high-temperature superconductivity in a specific nickelate compound [18]. More broadly speaking, the appearance of pairing is conventionally tied to the distortion of some underlying order. In the aforementioned example, it is the distortion of the underlying AFM order that gives rise to the induced attraction [19, 20], which is then further enhanced by restricting motion to one dimension. In conventional superconductors, electrons distort the underlying crystal lattice, inducing an attraction between them [21–23]. In materials supporting high-temperature superconductivity, there may be an important counterexample to this generic scenario, in which preformed Cooper pairs [24, 25] appearing above the superconducting phase transition might explain [26, 27] the pseudogap phase [28].

In this Letter, we demonstrate a pairing mechanism that *does not* rely on being in nor in the vicinity of a phase transition to an ordered phase. In particular, the discovered mechanism remains at *infinite* temperatures and is a direct consequence of the thermally disordered spin lattice. I analyze the effect in a simplistic setup of a mixed-dimensional model [Fig. 1(a)], where two holes

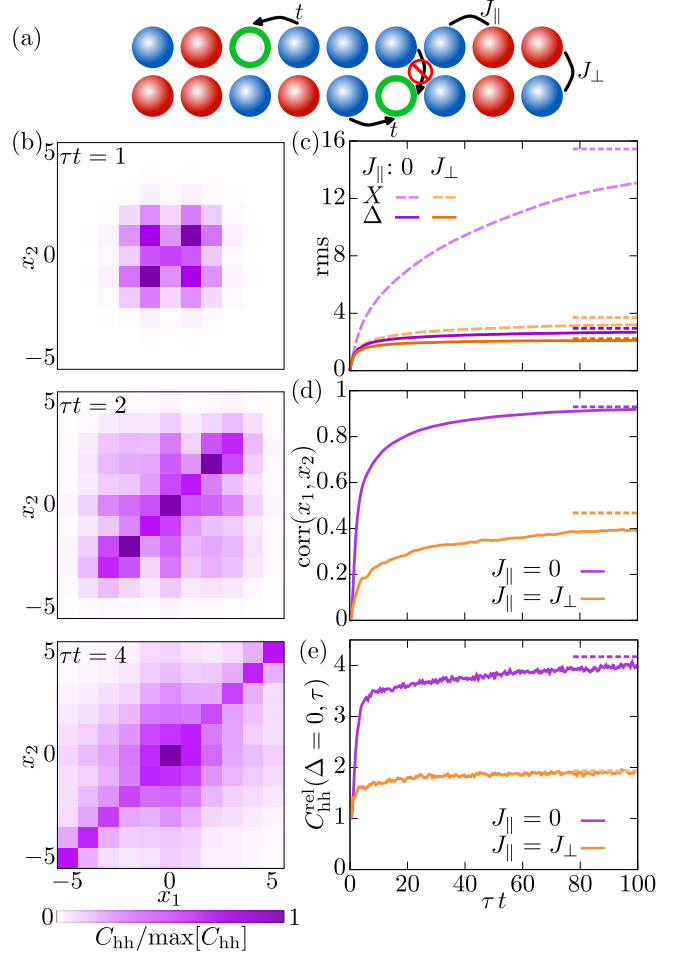


FIG. 1. **Pairing dynamics.** (a) Setup: holes move in a magnetic (red: \uparrow , blue: \downarrow) two-leg ladder with Ising interactions J_{\perp}, J_{\parallel} via nearest-neighbor hopping t along the ladder. (b) Hole-hole correlator $C_{hh}(x_1, x_2; \tau) = \langle \hat{n}_h(x_1) \hat{n}_h(x_2) \rangle_{\tau}$ for $J_{\parallel} = 0$ at indicated times normalized to its maximum after the holes are initialized on the same rung, $(l, x_1) = (1, 0), (l, x_2) = (2, 0)$. (c) Dynamics of the root-mean-square dynamics of the center-of-mass $X = (x_1 + x_2)/2$ and relative $\Delta = (x_1 - x_2)/2$ coordinates, (d) correlation coefficient $\text{corr}(x_1, x_2) = \langle x_1 x_2 \rangle_{\tau} / [\sigma(x_1) \sigma(x_2)]$, and (e) relative correlation function for $\Delta = 0$. Steady state values are shown in short dashed lines. In all: $J_{\perp} = 5t$.

are placed in two legs of a spin ladder. The spin degree of freedom is assumed to be at infinite temperature and completely disordered. Conventional wisdom, therefore, suggests that the holes should not be able to pair. Nevertheless, when the holes are initialized on the same rung in the infinite temperature spin lattice, the strong thermal disorder of the system frustrates the relative motion of the dopants. Indeed, tracking the hole-hole correlator in time [Fig. 1(b)], shows a significant correlation along the diagonal $x_1 = x_2$, where the holes are on the same rung of the ladder. One may equivalently observe that the inter-hole distance is always smaller than the traversed distance of their center-of-mass [Fig. 1(c)]. This results in a strictly *positive* correlation between the holes' position, signaling an effective attraction between them [Fig. 1(d)]. Finally, we observe that the probability of finding the holes on the same rung is easily increased by a factor of 4 as compared to what one expects from their marginal distributions, described by the relative hole-hole correlator in Fig. 1(e). This phenomenon is closely tied to the recent discovery of thermally induced localization in such systems [29, 30]. In particular, the holes experience an effective induced interaction that has a disordered character, encouraging the holes to co-propagate. I emphasize that the discovered effect would appear in a wide range of systems, though the robustness of the pairing in more generic setups is presently unclear.

Model.- I consider spins in a two-leg ladder with Ising interactions and hopping *along* the ladder,

$$\hat{H} = \sum_{\mathbf{i}, \mathbf{j}} \frac{J_{\mathbf{i}-\mathbf{j}}}{2} \hat{S}_{\mathbf{i}}^{(z)} \hat{S}_{\mathbf{j}}^{(z)} - t \sum_{\langle \mathbf{i}, \mathbf{j} \rangle_{\parallel}, \sigma} \left[\hat{c}_{\sigma \mathbf{i}}^{\dagger} \tilde{c}_{\sigma \mathbf{j}} + \tilde{c}_{\sigma \mathbf{j}}^{\dagger} \hat{c}_{\sigma \mathbf{i}} \right], \quad (1)$$

i.e. a mixed-dimensional t - J_z model [31]. I focus on the case of nearest-neighbor couplings along, $J_{\parallel} = J_{\pm \mathbf{e}_x}$, and across, $J_{\perp} = J_{\pm \mathbf{e}_y}$, the ladder, with $\hat{S}_{\mathbf{i}}^{(z)}$ the z -projection of the spin operator $\hat{\mathbf{S}}_{\mathbf{i}}$. The hopping, \hat{H}_t , is only allowed along the ladder and only to vacant sites, enforced by the constrained operators $\tilde{c}_{\sigma \mathbf{i}}^{\dagger} = \hat{c}_{\sigma \mathbf{i}}^{\dagger} [1 - \hat{n}_{\mathbf{i}}]$, where $\hat{n}_{\mathbf{i}} = \sum_{\sigma} \hat{n}_{\sigma \mathbf{i}} = \sum_{\sigma} \hat{c}_{\sigma \mathbf{i}}^{\dagger} \hat{c}_{\sigma \mathbf{i}}$ is the local density operator. The effective spin degree of freedom generally describes an internal degree of freedom with the Ising-type coupling in \hat{H}_J , the first term in Eq. (1), and since there are no exchange processes of the dopants, both fermions and bosons can realize the model. To have an efficient description of the hole and spin degrees of freedom, we perform a Holstein-Primakoff transformation on top of the *ferromagnetic* ground state $|\text{FM}\rangle = |\cdots \uparrow \uparrow \cdots\rangle$, with all spins in the $|\uparrow\rangle$ state. The spin Hamiltonian

$$\hat{H}_J = \sum_{\mathbf{i}, \mathbf{j}} \frac{J_{\mathbf{i}-\mathbf{j}}}{2} \left[\frac{1}{2} - \hat{s}_{\mathbf{i}}^{\dagger} \hat{s}_{\mathbf{i}} \right] \left[\frac{1}{2} - \hat{s}_{\mathbf{j}}^{\dagger} \hat{s}_{\mathbf{j}} \right] \left[1 - \hat{h}_{\mathbf{i}}^{\dagger} \hat{h}_{\mathbf{i}} \right] \left[1 - \hat{h}_{\mathbf{j}}^{\dagger} \hat{h}_{\mathbf{j}} \right], \quad (2)$$

hereby, describes the interaction of bosonic spin flip excitations $\hat{s}_{\mathbf{i}}^{\dagger}$, corresponding to the creation of a spin- \downarrow on site \mathbf{i} , and holes created by the operator $\hat{h}_{\mathbf{i}}^{\dagger}$, which inherit

the statistics of the underlying particles, be it fermionic or bosonic [20]. Equivalently, the hopping Hamiltonian

$$\hat{H}_t = t \sum_{\langle \mathbf{i}, \mathbf{j} \rangle_{\parallel}} \left[\hat{h}_{\mathbf{j}}^{\dagger} F(\hat{h}_{\mathbf{i}}, \hat{s}_{\mathbf{i}}) F(\hat{h}_{\mathbf{j}}, \hat{s}_{\mathbf{j}}) \hat{h}_{\mathbf{i}} + \hat{h}_{\mathbf{j}}^{\dagger} \hat{s}_{\mathbf{i}}^{\dagger} F(\hat{h}_{\mathbf{i}}, \hat{s}_{\mathbf{i}}) F(\hat{h}_{\mathbf{j}}, \hat{s}_{\mathbf{j}}) \hat{s}_{\mathbf{j}} \hat{h}_{\mathbf{i}} \right] + \text{H.c.} \quad (3)$$

describes two distinct ways in which holes may hop: (1) a hole hopping from site \mathbf{i} to \mathbf{j} in the absence of a spin flip on site \mathbf{j} , and (2) hopping in the presence of a spin flip, whereby the hole and spin flip swap places. The constraint function $F(\hat{h}, \hat{s}) = \sqrt{1 - \hat{s}^{\dagger} \hat{s} - \hat{h}^{\dagger} \hat{h}}$ ensures at most one spin per site. The initial state at time $\tau = 0$ of two holes on the same rung of the ladder in a spin background σ is then

$$|\Psi_{\sigma}(\tau = 0)\rangle = \prod_{l=1}^2 \hat{h}_{(l,0)}^{\dagger} \prod_{j \in S_{\sigma}^l} \hat{s}_{(l,j)}^{\dagger} |\text{FM}\rangle, \quad (4)$$

in which S_{σ}^l is the subset of spins in leg l , which are initially in the $|\downarrow\rangle$ state. Here, we write $\mathbf{i} = (l, j)$, with leg index $l = 1, 2$ and position j along the leg. Since the spins can only exchange places with the holes along the ladder, the state at any later stage is

$$|\Psi_{\sigma}(\tau)\rangle = \sum_{x_1, x_2} a_{\sigma}(x_1, x_2; \tau) \prod_{l=1}^2 \hat{h}_{(l, x_l)}^{\dagger} \times \prod_{\substack{j \in S_{\sigma}^l \\ j \in [\text{sgn}(x_l), x_l]}} \hat{s}_{(l, j - \text{sgn}(x_l))}^{\dagger} \prod_{\substack{j \in S_{\sigma}^l \\ j \notin [\text{sgn}(x_l), x_l]}} \hat{s}_{(l, j)}^{\dagger} |\text{FM}\rangle. \quad (5)$$

Here, $\text{sgn}(x)$ is the sign function. Despite the rather formal description, the physics is simple and clear: if the hole in leg l moves $|x_l|$ times to the right, it surpasses $|x_l|$ spins that all move one step to the left. If the hole moves to the left, the surpassed spins move one step to the right. The corresponding probability amplitudes $a_{\sigma}(x_1, x_2; \tau)$ of finding the holes at positions x_1, x_2 at time τ , follow the equations of motion

$$i\partial_{\tau} a_{\sigma}(x_1, x_2; \tau) = V_{\sigma}(x_1, x_2) a_{\sigma}(x_1, x_2; \tau) + t \sum_{\substack{\delta_1, \delta_2 \\ |\delta_1| + |\delta_2| = 1}} a_{\sigma}(x_1 + \delta_1, x_2 + \delta_2; \tau), \quad (6)$$

derived from the Schrödinger equation, $i\partial_{\tau} |\Psi_{\sigma}(\tau)\rangle = \hat{H} |\Psi_{\sigma}(\tau)\rangle$, with the initial condition that holes are on the same rung: $a_{\sigma}(x_1 = 0, x_2 = 0; \tau = 0) = 1$. The sum extends over configurations reached in a single hop. The induced interaction $V_{\sigma}(x_1, x_2)$ emerges, because the motion of the holes alter the spin bonds in the ladder [Fig. 2(a)]. For a random spin background, the induced interaction is also random [Fig. 2(b)], characterized in the relative and center-of-mass coordinates $\Delta = (x_1 - x_2)/2$ and $X = (x_1 + x_2)/2$. I indeed show [32] that if all spin

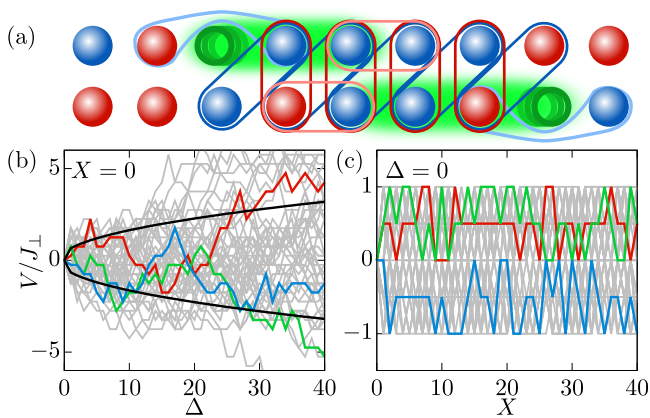


FIG. 2. **Pairing mechanism.** (a) As the holes move (green shaded region), spin bonds in the initial configuration are broken across (dark blue) and within (light blue) the ladder, and new bonds are established (dark and light red, respectively), resulting in a random induced interaction between the holes. (b) Induced interaction for vanishing center-of-mass, $X = 0$, as a function of the relative coordinate Δ for 50 realizations of the spin background (grey and colored lines), performing a random walk with standard deviation $\sim |J_{\perp}| \sqrt{|\Delta|}$ (black lines). (c) Induced interaction at $\Delta = 0$, as a function of X . Here, $J_{\parallel} = J_{\perp}$ is used.

backgrounds are equally likely – as in an infinite temperature spin state – $V_{\sigma}(x_1, x_2)$ has zero mean and a variance ($x_1, x_2 \neq 0$)

$$\text{Var}[V_{\sigma}(x_1, x_2)] = \frac{J_{\perp}^2}{4} \left[|\Delta| - \frac{1}{4} \right] + \frac{J_{\parallel}^2}{4} \quad (7)$$

linear in the relative distance $2|\Delta|$ between the holes, describing a classical random walk in the values of the potential [Fig. 2(b)]. I can focus on the evolution in specific spin backgrounds by resolving the dynamics of the density matrix in terms of these states. Starting from the initial density matrix

$$\hat{\rho}(\tau = 0) = \sum_{l=1,2,\sigma(l,0)} \hat{c}_{(l,0)\sigma(l,0)} \hat{\rho}_J \hat{c}_{(l,0)\sigma(l,0)}^{\dagger}, \quad (8)$$

where $\hat{\rho}_J = e^{-\beta \hat{H}_J} / Z_J$ is the Gibbs state of the spins at inverse temperature $\beta = 1/(k_B T)$ and $\sigma(l,0) = \uparrow, \downarrow$ designates the spin configuration at the origin of each leg, l , the ensuing dynamics $\hat{\rho}(\tau) = e^{-i\hat{H}\tau} \hat{\rho}(\tau = 0) e^{+i\hat{H}\tau}$ – provided that the system is assumed to be closed – is the Boltzmann-weighted sum [29, 30]

$$\hat{\rho}(\tau) = \sum_{\sigma} \frac{e^{-\beta E_J(\sigma)}}{Z_J} |\Psi_{\sigma}(\tau)\rangle \langle \Psi_{\sigma}(\tau)|, \quad (9)$$

where $E_J(\sigma)$ is the magnetic energy of the spin realization σ before the spins $\sigma_{(1,0)}, \sigma_{(2,0)}$ are removed. In particular, at infinite temperatures all pure state evolutions $|\Psi_{\sigma}(\tau)\rangle$ are sampled with equal probability,

$e^{-\beta E_J(\sigma)} / Z_J = 2^{-N}$, for system size N . In this high-temperature limit, the dynamics is exactly the same for antiferromagnetic ($J_{\perp}, J_{\parallel} > 0$) and ferromagnetic couplings ($J_{\perp}, J_{\parallel} < 0$). The calculation of the hole dynamics then follows the recipe: (1) generate a sample S of $N_S = 400$ random spin configurations σ and calculate $V_{\sigma}(x_1, x_2)$, (2) solve the equations of motion in Eq. (6) using exact diagonalization for $N = 161 \times 2$, and (3) compute the hole-hole correlator

$$C_{\text{hh}}(x_1, x_2; \tau) = \langle \hat{n}_h(x_1) \hat{n}_h(x_2) \rangle_{\tau} = \sum_{\sigma \in S} \frac{|a_{\sigma}(x_1, x_2; \tau)|^2}{N_S}, \quad (10)$$

whereby it may be tracked in time [Fig. 1(b)]. This describes the probability of simultaneously finding holes at positions $(1, x_1), (2, x_2)$. Here, $\hat{n}_h(x_l) = \hat{h}_{(l,x_l)}^{\dagger} \hat{h}_{(l,x_l)}$ is the hole density operator. Figure 1(b) manifestly breaks the individual inversion symmetries $x_1 \rightarrow -x_1$ or $x_2 \rightarrow -x_2$ of uncorrelated holes, and shows a clear tendency for them to be on the same rung ($x_1 = x_2 \Leftrightarrow \Delta = 0$). Their motion is further analyzed by the root-mean-square of the center-of-mass and relative coordinates [Fig. 1(c)],

$$A_{\text{rms}}(\tau) = \left[\sum_{X,\Delta} A^2 C_{\text{hh}}(X + \Delta, X - \Delta; \tau) \right]^{1/2}, \quad (11)$$

for $A = X, \Delta$. Since $X_{\text{rms}} > \Delta_{\text{rms}}$, the holes are closer together than they have propagated into the lattice. This is further characterized by the correlation coefficient

$$\text{corr}(x_1, x_2) = \frac{\langle x_1 x_2 \rangle_{\tau}}{\sigma(x_1) \sigma(x_2)} = \frac{X_{\text{rms}}^2 - \Delta_{\text{rms}}^2}{X_{\text{rms}}^2 + \Delta_{\text{rms}}^2}, \quad (12)$$

which is always restricted to the interval $[-1, +1]$. Positive values of $\text{corr}(x_1, x_2)$, as seen in Fig. 1(d), correspond to $X_{\text{rms}} > \Delta_{\text{rms}}$, and signify *attraction*. Likewise, negative values correspond to an effective repulsion, while $\text{corr}(x_1, x_2) = 0$ corresponds to no linear correlations. To further substantiate the findings, I analyze the relative hole-hole correlator

$$C_{\text{hh}}^{\text{rel}}(\Delta, \tau) = \frac{\sum_X C_{\text{hh}}(X + \Delta, X - \Delta; \tau)}{\sum_X C_{\text{hh}}^{\text{disc}}(X + \Delta, X - \Delta; \tau)}, \quad (13)$$

giving the probability of finding the holes at distance $2|\Delta|$ relative to what is expected from their marginals, i.e. the disconnected correlator $C_{\text{hh}}^{\text{disc}}(\Delta, \tau) = \sum_X \langle \hat{n}_h(X + \Delta) \rangle \langle \hat{n}_h(X - \Delta) \rangle$. This is shown for $\Delta = 0$ in Fig. 1(e), demonstrating a significant increase in the probability of finding the holes on the same rung. On long timescales, the system settles into a steady state, by which $X_{\text{rms}} \rightarrow l_X, \Delta_{\text{rms}} \rightarrow l_{\Delta}$. For $J_{\perp} \geq 2t$, there are negligible finite-size corrections for the chosen length of $N/2 = 161$, and I, therefore, confine the analysis to this regime. Figure 3(a), hereby, shows that $l_X > l_{\Delta}$ remains true over this entire range of parameters. The associated asymptote of the correlation coefficient [Fig. 3(b)]

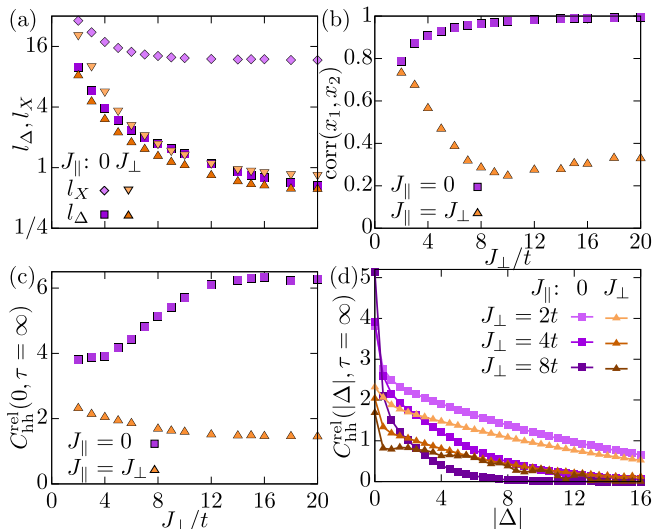


FIG. 3. **Steady state.** (a) The rms distances l_X and l_Δ of the center-of-mass, X , and relative, Δ , coordinates of the holes as a function of J_\perp/t for indicated values of J_\parallel in the steady state. (b) Associated correlation coefficient $\text{corr}(x_1, x_2) = \langle \sigma(x_1)\sigma(x_2) \rangle / [\sigma(x_1)\sigma(x_2)]$. (c) Relative hole-hole correlator [Eq. (13)] for holes on the same rung ($\Delta = 0$) vs J_\perp/t . (d) Relative hole-hole correlator vs $|\Delta|$ for indicated values of J_\perp/t and J_\parallel .

shows very strong attractive correlations for $J_\perp \gg t$ and $J_\parallel = 0$. The dynamical binding – a finite l_Δ – has the *exact* same origin as the thermal localization phenomenon discovered recently for the motion of single holes [29, 30], by which the separation of the holes is avoided, because the induced interaction $V_\sigma(x_1, x_2)$ inevitably fluctuates to large values in the relative distance $2|\Delta| = |x_1 - x_2|$, as seen in Fig. 2(b). Therefore, at the very least, they back-reflect once they meet their classical turning points, corresponding to an emergent kind of Anderson localization [33] in the presence of *strong disorder* [34]. The retained localization of the holes – a finite l_X – is more subtle, because $V_\sigma(x, x)$ is restricted to take values between $\pm|J_\parallel|$ [Fig. 2(c)], such that it vanishes for holes on the same rung in the extreme limit of $J_\parallel = 0$. Even in this case, however, the holes localize [Fig. 3(b)]. The reason is that there are many ways in which the holes can move to sites $(1, x)$ and $(2, x)$. Along each path, the wave builds up a phase directly depending on the randomly fluctuating induced interaction they meet along the way. The ensuing destructive interference of these pathways corresponds to Anderson localization for *weak* disorder [34]. Finally, the relative hole-hole correlator in Figs. 3(c) and 3(d) show that the probability of finding holes in close proximity can be several times higher than expected from their marginals. Overall, it is clear that at large J_\perp/t the strength of the pairing sensitively depends on J_\parallel , essentially because the holes localize over very few lattice sites if $J_\parallel \sim J_\perp$. However, already at intermediate values of J_\perp/t , the pairing for $J_\parallel = J_\perp$ is comparable to the case of $J_\parallel = 0$. I expect this to persist at lower J_\perp/t .

Rydberg-dressed atoms.– The predicted results may be feasibly tested in ultracold quantum simulators based on Rydberg-dressed atoms in optical lattices [35]. Indeed, such schemes natively realizes spin-specific density-density interactions

$$\hat{H}_J = \frac{1}{2} \sum_{i \neq j} J_{i-j} \hat{n}_{i\uparrow} \hat{n}_{j\uparrow} \quad (14)$$

of the internal atomic state $|\uparrow\rangle$, by optically dressing it with a higher-lying Rydberg state. Here, J_{i-j} takes on a soft core shape [32, 36]. Moreover, such systems were recently demonstrated to enter the itinerant regime [16], by which the desired t - J model may be realized. In particular, the spin model in Eq. (14) is obtained by using a Feshbach resonance to enhance the onsite interaction deep into the Mott-insulating phase. This ensures at most one spin per site and negligible spin superexchange. Precise control of the temperature in such systems is difficult, but the hole dynamics may still be investigated in the following manner [29]. First, initialize holes at $x_1 = x_2 = 0$ by applying a strong repulsive light field to those sites [6]. Second, rotate all spins from the fully polarized spin sample in the non-interacting $|\downarrow\rangle$ state into the equal superposition state $|\Psi_0\rangle = \prod_{i \neq 0} \frac{1}{\sqrt{2}} [\hat{c}_{i\uparrow}^\dagger + \hat{c}_{i\downarrow}^\dagger] |0\rangle$. Third, turn off the focused light fields, freeing the holes to move along the ladder [12]. Although this at face value seems distinct from the infinite temperature scenario above, the hole-hole correlator takes on the exact same form

$$C_{\text{hh}}(x_1, x_2; \tau) = 2^{-N} \sum_{\sigma} |a_\sigma(x_1, x_2; \tau)|^2, \quad (15)$$

such that the holes move as though the system is at infinite temperature. The polarized Ising form of the interaction is crucial for this exact equivalence, and one should note that *spin* correlators would presumably differ from their infinite temperature counterpart. The computation now follows the same recipe as before, and the resulting correlation coefficient dynamics [Eq. (12)] and relative correlation function [Eq. (13)] are given in Figs. 4(a) and 4(b), respectively. This is averaged over $N_S = 1000$ realizations and given in two instances [inset of Fig. 4(a)]: (1) isotropic couplings akin to the $J_\parallel = J_\perp$ case, and (2) anisotropic couplings where the $30P_{3/2}$ orbital of the Rydberg state is rotated to lie along the rungs using an external magnetic field [35], suppressing coupling in other directions similar to low values of J_\parallel [32]. Crucially, we observe that the appearing disorder-induced attraction between the holes can be probed for experimentally feasible system sizes *and* timescales. Indeed, stroboscopic dressing [16] makes 20 tunneling events feasible, while longer timescales are inhibited by the intrinsic lifetime of the Rydberg state [37]. I note that the rung case gives a much more favorable signal, just as was the case for $J_\parallel = 0$ vs $J_\parallel = J_\perp$.

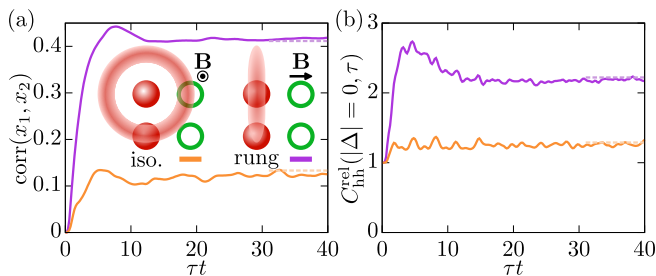


FIG. 4. **Rydberg dressing.** (a) Dynamics of the correlation coefficient for isotropic (orange) and strong rung (purple) spin couplings. (b) Associated relative correlator for holes on the same rung, $\Delta = 0$. Dashed lines: steady state values. Nearest neighbor rung interaction: $J_{e_y} = 8t$. Insets: orientation of $30P_{3/2}$ Rydberg orbitals enforced by shown magnetic fields \mathbf{B} . System size: $N = 21 \times 2$.

Conclusions and outlook.- I have demonstrated that thermal disorder of spins can frustrate the relative motion of dopants and lead to a dynamical pairing mechanism. The effect is closely related to the thermally induced localization phenomenon recently discovered for single holes [29, 30]. By carefully analyzing its origin and behavior at infinite temperature, it is, furthermore, clear that the effect persists for all values of the spin coupling versus the hopping. For diminishing temperatures, ferromagnetic interaction is expected to lead to a crossover to delocalized and uncorrelated holes. For antiferromagnetic interactions, on the other hand, a crossover from fluctuation induced pairing to *confinement* of the holes emerges at low temperatures [20]. Moreover, it demonstrates that the localization phenomenon [29, 30] is *not* sensitive to further doping. The results finally show that it is feasible to experimentally test my predictions using currently available techniques with ultracold atoms in optical lattices. One could also engineer similar models using Rydberg arrays [38–42] or polar molecules [43]. In the future, the generality of the discovered effect may be tested by, e.g., tuning in trans-leg hopping or spin superexchange. The robustness of the phenomenon to such alterations is presently unclear. The nature of the effect is, however, very general – it comes down to a randomly fluctuating field emerging as the dopants separate, frustrating their relative motion.

The author thanks Pascal Weckesser, Johannes Zeiher, Pavel Kos, and J. Ignacio Cirac for helpful input and discussions. A special thanks goes to Pascal Weckesser for computing the soft core potentials. This work has been supported by the Carlsberg Foundation through a Carlsberg Internationalisation Fellowship, Grant No. CF21.0410.

- [1] J. R. Schrieffer and J. S. Brooks, *Handbook of high-temperature superconductivity* (Springer, 2007).
- [2] S. A. Trugman, Phys. Rev. B **37**, 1597 (1988).
- [3] E. Dagotto, Rev. Mod. Phys. **66**, 763 (1994).
- [4] S. M. O’Mahony, W. Ren, W. Chen, Y. X. Chong, X. Liu, H. Eisaki, S. Uchida, M. H. Hamidian, and J. C. S. Davis, Proceedings of the National Academy of Sciences **119**, e2207449119 (2022).
- [5] C. Gross and I. Bloch, Science **357**, 995 (2017).
- [6] G. Ji, M. Xu, L. H. Kendrick, C. S. Chiu, J. C. Brüggenjürgen, D. Greif, A. Bohrdt, F. Grusdt, E. Demler, M. Lebrat, and M. Greiner, Phys. Rev. X **11**, 021022 (2021).
- [7] Y. Wang, A. Bohrdt, S. Ding, J. Koepsell, E. Demler, and F. Grusdt, Phys. Rev. Research **3**, 033204 (2021).
- [8] M. L. Prichard, B. M. Spar, I. Morera, E. Demler, Z. Z. Yan, and W. S. Bakr, “Directly imaging spin polarons in a kinetically frustrated hubbard system,” (2023), arXiv:2308.12951 [cond-mat.quant-gas].
- [9] J. Koepsell, J. Vijayan, P. Sompet, F. Grusdt, T. A. Hilker, E. Demler, G. Salomon, I. Bloch, and C. Gross, Nature **572**, 358 (2019).
- [10] J. Koepsell, D. Bourgund, P. Sompet, S. Hirthe, A. Bohrdt, Y. Wang, F. Grusdt, E. Demler, G. Salomon, C. Gross, and I. Bloch, Science **374**, 82 (2021).
- [11] M. Lebrat, M. Xu, L. H. Kendrick, A. Kale, Y. Gang, P. Seetharaman, I. Morera, E. Khatami, E. Demler, and M. Greiner, Nature **629**, 317 (2024).
- [12] S. Hirthe, T. Chalopin, D. Bourgund, P. Bojović, A. Bohrdt, E. Demler, F. Grusdt, I. Bloch, and T. A. Hilker, Nature **613**, 463 (2023).
- [13] W. S. Bakr, J. I. Gillen, A. Peng, S. Fölling, and M. Greiner, Nature **462**, 74 (2009).
- [14] J. F. Sherson, C. Weitenberg, M. Endres, M. Cheneau, I. Bloch, and S. Kuhr, Nature **467**, 68 (2010).
- [15] K. K. Nielsen, T. Pohl, and G. M. Bruun, Phys. Rev. Lett. **129**, 246601 (2022).
- [16] P. Weckesser, K. Srakaew, T. Blatz, D. Wei, D. Adler, S. Agrawal, A. Bohrdt, I. Bloch, and J. Zeiher, “Realization of a rydberg-dressed extended bose hubbard model,” (2024), arXiv:2405.20128 [cond-mat.quant-gas].
- [17] H. Schlömer, U. Schollwöck, F. Grusdt, and A. Bohrdt, “Superconductivity in the pressurized nickelate $\text{La}_3\text{Ni}_2\text{O}_7$ in the vicinity of a bec-bcs crossover,” (2023), arXiv:2311.03349 [cond-mat.str-el].
- [18] H. Sun, M. Huo, X. Hu, J. Li, Z. Liu, Y. Han, L. Tang, Z. Mao, P. Yang, B. Wang, J. Cheng, D.-X. Yao, G.-M. Zhang, and M. Wang, Nature **621**, 493 (2023).
- [19] A. Bohrdt, L. Homeier, I. Bloch, E. Demler, and F. Grusdt, Nature Physics **18**, 651 (2022).
- [20] K. K. Nielsen, Phys. Rev. B **108**, 085125 (2023).
- [21] H. Fröhlich, Phys. Rev. **79**, 845 (1950).
- [22] J. Bardeen, L. N. Cooper, and J. R. Schrieffer, Phys. Rev. **108**, 1175 (1957).
- [23] H. Bruus and K. Flensberg, *Many-body quantum theory in condensed matter physics – an introduction* (Oxford University Press, 2016).
- [24] V. B. Geshkenbein, L. B. Ioffe, and A. I. Larkin, Phys. Rev. B **55**, 3173 (1997).
- [25] M. Randeria, N. Trivedi, A. Moreo, and R. T. Scalettar, Phys. Rev. Lett. **69**, 2001 (1992).

- [26] L. Li, Y. Wang, S. Komiya, S. Ono, Y. Ando, G. D. Gu, and N. P. Ong, *Phys. Rev. B* **81**, 054510 (2010).
- [27] Y. I. Seo, W. J. Choi, S.-i. Kimura, and Y. S. Kwon, *Scientific Reports* **9**, 3987 (2019).
- [28] T. D. Stanescu and P. Phillips, *Phys. Rev. Lett.* **91**, 017002 (2003).
- [29] K. K. Nielsen, *Phys. Rev. Res.* **6**, 023325 (2024).
- [30] K. K. Nielsen, “Localized dopant motion across the 2d ising phase transition,” (2024), arXiv:2404.11608 [cond-mat.str-el].
- [31] F. Grusdt and L. Pollet, *Phys. Rev. Lett.* **125**, 256401 (2020).
- [32] See Supplemental Material online for additional details.
- [33] P. W. Anderson, *Phys. Rev.* **109**, 1492 (1958).
- [34] A. Lagendijk, B. v. Tiggelen, and D. S. Wiersma, *Physics Today* **62**, 24 (2009).
- [35] J. Zeiher, R. van Bijnen, P. Schauß, S. Hild, J.-y. Choi, T. Pohl, I. Bloch, and C. Gross, *Nature Physics* **12**, 1095 (2016).
- [36] N. Henkel, R. Nath, and T. Pohl, *Phys. Rev. Lett.* **104**, 195302 (2010).
- [37] P. Weckesser, Private Communication (2024).
- [38] P. Schauss, J. Zeiher, T. Fukuhara, S. Hild, M. Cheneau, T. Macrì, T. Pohl, I. Bloch, and C. Gross, *Science* **347**, 1455 (2015).
- [39] H. Labuhn, D. Barredo, S. Ravets, S. de Léséleuc, T. Macrì, T. Lahaye, and A. Browaeys, *Nature* **534**, 667 (2016).
- [40] H. Bernien, S. Schwartz, A. Keesling, H. Levine, A. Omran, H. Pichler, S. Choi, A. S. Zibrov, M. Endres, M. Greiner, V. Vuletić, and M. D. Lukin, *Nature* **551**, 579 (2017).
- [41] E. Guardado-Sanchez, P. T. Brown, D. Mitra, T. Devakul, D. A. Huse, P. Schauß, and W. S. Bakr, *Phys. Rev. X* **8**, 021069 (2018).
- [42] V. Lienhard, S. de Léséleuc, D. Barredo, T. Lahaye, A. Browaeys, M. Schuler, L.-P. Henry, and A. M. Läuchli, *Phys. Rev. X* **8**, 021070 (2018).
- [43] A. V. Gorshkov, S. R. Manmana, G. Chen, J. Ye, E. Demler, M. D. Lukin, and A. M. Rey, *Phys. Rev. Lett.* **107**, 115301 (2011).

Supplemental Material

Pairing by disorder of dopants in magnetic spin ladder

CONTENTS

Induced interaction of two holes	1
Soft core potential	2
References	4

INDUCED INTERACTION OF TWO HOLES

In this section, I write down the explicit induced interaction of two holes for a specific spin realization σ . The role of this potential is that it directly enters the equations of motion for said spin realization,

$$i\partial_\tau a_\sigma(x_1, x_2; \tau) = V_\sigma(x_1, x_2) a_\sigma(x_1, x_2; \tau) + t [a_\sigma(x_1 - 1, x_2; \tau) + a_\sigma(x_1 + 1, x_2; \tau) + a_\sigma(x_1, x_2 - 1; \tau) + a_\sigma(x_1, x_2 + 1; \tau)], \quad (\text{S1})$$

as the effective local energy shift of the two holes at positions (x_1, x_2) . As we shall shortly see, there are two special features of this interaction: (1) it is not translationally invariant for general σ , (2) it favors the holes to co-propagate. As for the single-hole case [1], I separate the potential into parts coming from the intra-leg and trans-leg spin couplings: $V_\sigma = V_{\sigma, \parallel} + V_{\sigma, \perp}$. Here, $V_{\sigma, \parallel} \propto J_{\parallel}$ and $V_{\sigma, \perp} \propto J_{\perp}$.

For the intra-leg potential, there is no influence between the two holes. Therefore, the potential is simply the sum of two copies of the single hole case: $V_{\sigma, \parallel}(x_1, x_2) = V_{\sigma, \parallel}(x_1) + V_{\sigma, \parallel}(x_2)$, with [Ref. [1], Eq. (13)]

$$V_{\sigma, \parallel}(x_i) = J_{\parallel} \begin{cases} \sigma_{(i, -1)} \sigma_{(i, 1)} - \sigma_{(i, x_i)} \sigma_{(i, x_i + 1)}, & x_i > 0, \\ \sigma_{(i, -1)} \sigma_{(i, 1)} - \sigma_{(i, x_i)} \sigma_{(i, x_i - 1)}, & x_i < 0, \end{cases} \quad (\text{S2})$$

for $i = 1, 2$. From here, it is already clear that the potential is not translationally invariant.

The more interesting contribution comes from the trans-leg part, $V_{\sigma, \perp}$. The key observation here, is that if the holes have the same x -coordinate, sitting as nearest neighbors across the ladder, any changes in the spin couplings across the ladder has been repaired. This means that $V_{\sigma, \perp}(x, x) = 0$. It also means that the trans-leg potential *only* depends on the spins between the holes. More explicitly, when $x_1 \neq x_2$, we can first consider $x_1 < x_2$. Here, I break it up into three cases. First, for $x_2 > x_1 \geq 0$

$$V_{\sigma, \perp}(x_1, x_2) = J_{\perp} (1 - \delta_{x_2, x_1 + 1}) \sum_{j=x_1+1}^{x_2-1} \sigma_{(1, j)} [\sigma_{(2, j+1)} - \sigma_{(2, j)}] - J_{\perp} \sigma_{(1, x_2)} \sigma_{(2, x_2)}. \quad (\text{S3})$$

The Kronecker δ term is there to prevent a contribution from the sum in the case that $x_2 = x_1 + 1$. Second, for $x_2 > 0 > x_1$

$$V_{\sigma, \perp}(x_1, x_2) = J_{\perp} (1 - \delta_{x_2, x_1 + 1}) \sum_{j=1}^{x_2-1} \sigma_{(1, j)} [\sigma_{(2, j+1)} - \sigma_{(2, j)}] - J_{\perp} \sigma_{(1, x_2)} \sigma_{(2, x_2)} + J_{\perp} (1 - \delta_{x_1, -1}) \sum_{j=x_1+1}^{-1} \sigma_{(2, j)} [\sigma_{(1, j-1)} - \sigma_{(1, j)}] - J_{\perp} \sigma_{(1, x_1)} \sigma_{(2, x_1)} + J_{\perp} \sigma_{(1, -1)} \sigma_{(2, -1)}. \quad (\text{S4})$$

Third, for $0 \geq x_2 > x_1$

$$V_{\sigma, \perp}(x_1, x_2) = J_{\perp} (1 - \delta_{x_2, x_1 + 1}) \sum_{j=x_1+1}^{x_2-1} \sigma_{(2, j)} [\sigma_{(1, j-1)} - \sigma_{(1, j)}] - J_{\perp} \sigma_{(1, x_1)} \sigma_{(2, x_1)}. \quad (\text{S5})$$

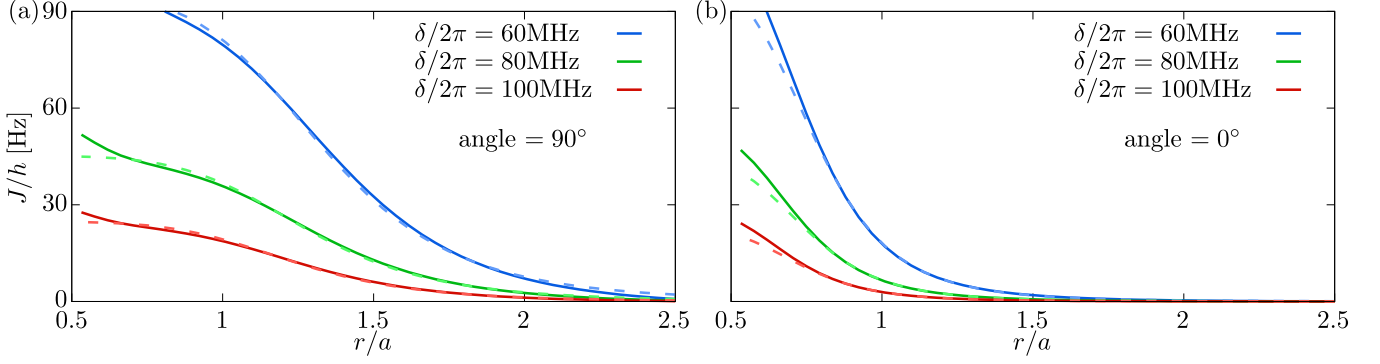


FIG. S1. (a) Interaction potential in units of Hz as a function of distance in units of the lattice spacing perpendicular to the direction of the applied magnetic field. This is shown for indicated values of the detuning, δ . The bigger the detuning, the smaller the overall energy scale, and the shorter the range of the interaction. (b) Same as in (a), but along the direction of the magnetic field. In the latter case, the potential falls off much more quickly. Dashed lines show approximate potentials by fitting to $J(r) = J_0/(1 + (r/r_c)^6)$.

For $x_1 > x_2$, we simply need to swap: $x_1 \leftrightarrow x_2$ and $\sigma_{(1,j)} \leftrightarrow \sigma_{(2,j)}$.

Finally, let us analyze the potential statistically. Since the spin lattice is assumed to be at infinite temperature, all spin correlation functions vanish: $\langle \sigma_i \sigma_j \rangle = 0$ for $\mathbf{i} \neq \mathbf{j}$. Therefore, the mean value of the induced interaction vanishes as well: $\langle V_{\sigma}(x_1, x_2) \rangle = \langle V_{\sigma, \parallel}(x_1, x_2) \rangle + \langle V_{\sigma, \perp}(x_1, x_2) \rangle = 0$. Moreover, the lack of correlations between sites mean that the variance only gets nonzero contributions from onsite terms: $\langle (\sigma_i \sigma_j)^2 \rangle = \langle \sigma_i^2 \sigma_j^2 \rangle = 1/16$. As a result, the variance of the intra-leg potential is simply

$$\text{Var}[V_{\sigma, \parallel}(x_1, x_2)] = \langle [V_{\sigma, \parallel}(x_1, x_2)]^2 \rangle = 2J_{\parallel}^2 [\langle (\sigma_{(1,-1)} \sigma_{(1,1)})^2 \rangle + \langle (\sigma_{(1,x_i)} \sigma_{(1,x_i+1)})^2 \rangle] = \frac{J_{\parallel}^2}{4}, \quad (\text{S6})$$

for $x_1, x_2 \neq 0$. If one is at its origin, the variance drops to $\frac{J_{\parallel}^2}{8}$, and if both are at the origin it vanishes. For the trans-leg potential, we may note that whenever $x_2 \neq x_1$, there is always $2|x_2 - x_1| - 1 = 4|\Delta| - 1$ terms of the form $\langle (\sigma_i \sigma_j)^2 \rangle = 1/16$. Therefore,

$$\text{Var}[V_{\sigma, \perp}(x_1, x_2)] = \frac{J_{\perp}^2}{16} [4|\Delta| - 1] = \frac{J_{\perp}^2}{4} \left[|\Delta| - \frac{1}{4} \right]. \quad (\text{S7})$$

The total variance is then [see also Eq. (7) of the main text]

$$\text{Var}[V_{\sigma}(x_1, x_2)] = \frac{J_{\perp}^2}{4} \left[|\Delta| - \frac{1}{4} \right] + \frac{J_{\parallel}^2}{4}, \quad (\text{S8})$$

whenever both x_1, x_2 are nonzero, and when $\Delta = x_1 - x_2 \neq 0$.

SOFT CORE POTENTIAL

The proposal for the experimental setup is based on Refs. [2, 3] using ^{87}Rb . The σ^+ transition between the $|F=2, m_F=2\rangle$ state in the $5S_{1/2}$ manifold and the $|J=3/2, m_J=3/2\rangle$ Rydberg state in the $30P_{3/2}$ manifold is *stroboscopically* driven with Rabi frequency Ω , detuning δ , and duty cycle $D = 1/600$. The assumed lattice spacing is $a = 752\text{nm}$, and I set $\Omega = 2\pi \times 20\text{MHz}$. I analyze the dynamics for three distinct experimentally feasible values of the detuning, $\delta = 2\pi \times 60\text{MHz}, 2\pi \times 80\text{MHz}, 2\pi \times 100\text{MHz}$. The pulsed scheme dramatically improves the lifetime of the Rydberg-dressed state, while the effective Hamiltonian describing the dynamics remains unchanged [3].

As a first step to calculate the interaction of the dressed atoms, one first needs the pair interaction of two pure Rydberg states $|rr\rangle$. This is performed using the open source code documented in Ref. [4]. As a next step, the Rabi coupling to these Rydberg states results in a dressing of the spin- $|\uparrow\rangle$ states, $|\tilde{\uparrow}\rangle$. As a result of the dressing, there is an effective interaction potential in the $|\tilde{\uparrow}\tilde{\uparrow}\rangle$ sector. This calculation was carried through by Pascal Weckesser and

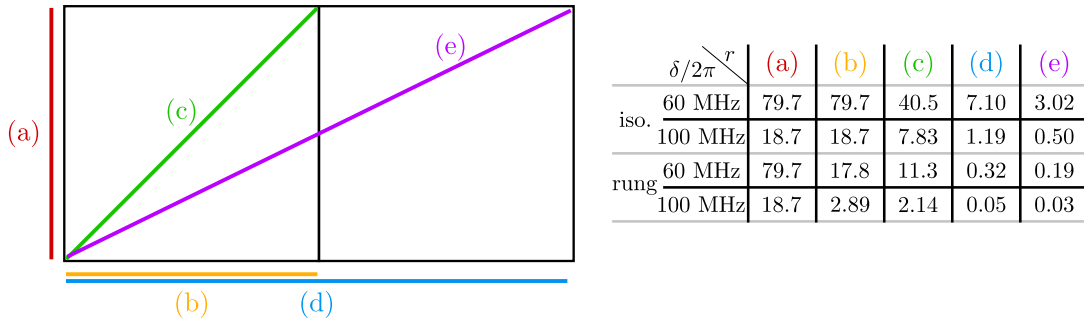


FIG. S2. The interaction potential is calculated (right) for the shown distances in the lattice (left). Beyond a distance of $\sqrt{5}$ lattice spacings (e), the potential is reduced by 3 orders of magnitude and neglected. The top two rows in the table refer to the isotropic case, where the magnetic field is perpendicular to the ladder. The lower two rows refer to the rung case, where the magnetic field is along the ladder, and the interaction is suppressed away from the rung.

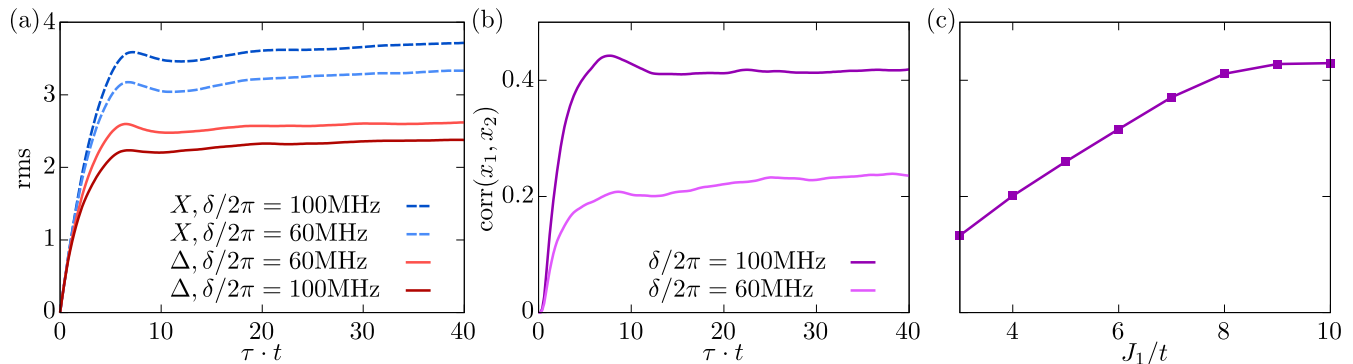


FIG. S3. (a) The rms dynamics of the center-of-mass, X , and relative, Δ , coordinates for indicated detunings, δ , and a magnetic field along the ladder (dominant rung coupling). Note that for lower detunings, the signal worsens both because the rms of the center-of-mass position decreases and because the relative distance increases. (b) The associated dynamics of the correlation coefficient showing much better visibility at larger detuning. (c) Asymptotic correlation coefficient vs $J_1 = J_{e_y}$.

follows the recipe given in the Supplementary Material of Ref. [2]. The resulting Hamiltonian [Eq. (14) of the main text]

$$\hat{H}_J = \frac{1}{2} \sum_{i \neq j} J_{i-j} \hat{n}_{\uparrow i} \hat{n}_{\uparrow j} \quad (\text{S9})$$

describes spin-specific density-density interactions. The behavior of this potential depends very much on the orientation of the electron orbital in the addressed $30P_{3/2}$ Rydberg state. This may be manipulated by applying a magnetic field, whose direction defines the quantization axis, and thereby, the orbital orientation. Indeed, the dependency of the potential, J_{i-j} , on the interparticle distance, $r = |\mathbf{i} - \mathbf{j}|$, is significantly different in the plane of the orbital (perpendicular to the magnetic field) [Fig. S1(a)], and along the applied magnetic field [Fig. S1(b)]. In the latter case, it falls off much more quickly. By putting the magnetic field *along* the ladder, one may then suppress the interaction in this direction, while the interaction along the rungs is unchanged. In Fig. S2, I show for which distances the interaction potential is calculated. In the isotropic case, all distance vectors are at a 90° angle with the magnetic field and these all follow from the calculation of the potential in Fig. S1(a). In the rung case, the magnetic field points along the ladder. The case (a) in Fig. S2 is hereby still at a 90° angle and gives the same result as in the isotropic case at that distance. However, cases (b) and (d) must be extracted from the 0° calculation, while cases (c) and (e) are extracted from calculations at 45° and 26.6° with respect to the magnetic field. Importantly, by increasing the detuning from $\delta = 60$ MHz to $\delta = 100$ MHz, the relative size of the interactions at distances (b) and (c) are decreased from $17.8/79.7 \simeq 0.22$, $11.3/79.7 \simeq 0.14$ to $2.89/18.7 \simeq 0.15$, $2.14/79.7 \simeq 0.11$, respectively. Although this is a minor change, this actually makes a big difference for the visibility of the results at the chosen system size of 21×2 . This is shown explicitly in Fig. S3. Figure S3(a) shows the rms distance of the center-of-mass and relative coordinates in the two cases. For $\Delta/2\pi = 100$ MHz, there is a much better separation of these two length scales. Indeed, Fig. S3(b) shows that the correlation coefficient is roughly doubled by going from $\Delta/2\pi = 60$ MHz to $\Delta/2\pi = 100$ MHz. In

these calculations, I assume that the strongest spin coupling (along the rung) is $J_1 = J_{e_y} = 8t$, as in the main text. This is achievable by adjusting the potential depth of the optical lattice, which is very much within experimental capabilities [3]. Finally, in Fig. S3(c), I show the asymptotic correlation coefficient for the chosen system size as a function of J_1/t . We see that it levels off around the chosen value of $J_1/t = 8$.

-
- [1] K. K. Nielsen, Phys. Rev. Res. **6**, 023325 (2024).
[2] J. Zeiher, R. van Bijnen, P. Schauß, S. Hild, J.-y. Choi, T. Pohl, I. Bloch, and C. Gross, Nature Physics **12**, 1095 (2016).
[3] P. Weckesser, K. Srakaew, T. Blatz, D. Wei, D. Adler, S. Agrawal, A. Bohrdt, I. Bloch, and J. Zeiher, “Realization of a rydberg-dressed extended bose hubbard model,” (2024), arXiv:2405.20128 [cond-mat.quant-gas].
[4] S. Weber, C. Tresp, H. Menke, A. Urvoy, O. Firstenberg, H. P. Büchler, and S. Hofferberth, Journal of Physics B: Atomic, Molecular and Optical Physics **50**, 133001 (2017).